Int J Earth Sci (Geol Rundsch) (2013) 102:121–138
DOI 10.1007/s00531-012-0794-z

ORIGINAL PAPER

Fault damage zone origin of the Teufelsmauer, Subhercynian Cretaceous Basin, Germany

Christian Klimczak · Richard A. Schultz

Received: 1 May 2012 / Accepted: 20 May 2012 / Published online: 9 June 2012

Abstract Recognition of fractures as porosity-reducing deformation bands pervading all sandstone segments of the Teufelsmauer, Subhercynian Creatceous Basin, Germany, motivates a study relating the observed macroscopic and microscopic deformation to the damage zone of the nearby Harz border fault. Deformation bands, confirmed and documented by several porosity-reducing micro-mechanisms, such as cataclasis, particulate flow, pressure solution and a heavy quartz cementation, were mapped and analyzed in terms of the kinematics and deformation intensities expressed by them. Deformation band kinematics are uniform throughout the entire basin and consistent with the large-scale tectonic structures of the area. A strain intensity study highlights two narrow but long zones of deformation bands, sub-parallel to the Harz border fault. Deformation band kinematics, strain intensity, as well as micro-mechanisms are all consistent with a continuous but internally diverse deformation band damage zone of the entire Teufelsmauer structure along the Harz border fault, bringing new insights into the tectonic evolution and the origin of the heavy quartz cementation of the sandstones in the Subhercynian Cretaceous Basin.

Keywords Harz Mountains · Deformation bands · Fault damage zone · Teufelsmauer

Introduction

The Harz Mountains and its foreland, the Subhercynian Cretaceous Basin (SCB), in central Germany (Fig. 1) is known for its myths and legends, which people passed on for generations in order to explain geologically enigmatic phenomena. Among these phenomena is Germany's oldest natural monument, the Teufelsmauer, meaning "Devil's Wall," of which the origin is still a subject of debate. The Teufelsmauer (Fig. 2) is a more than 30-km-long alignment of segments of hardened sandstone ridges and towers that morphologically stand out from otherwise unconsolidated sands of the SCB (Fig. 2a). Its origin has previously been attributed to the migration of silica-enriched fluids from depth due to hydrothermal activity, pore space infiltration driven by tectonic forces (Franzke et al. 2004, 2005) or groundwater hydraulic mechanisms (Voigt and Eynatten 2004, 2006). These scenarios explain origins for individual segments of the Teufelsmauer; however, they are not supported by further evidence at other segments of the structure. Gaining further insights on the origin of these narrow but widespread, consolidated sandstone ridges forming the Teufelsmauer is therefore desirable for understanding the controlling parameters of sandstone consolidation and diagenetic and fluid migration processes involved in such basins. Detailed background on the Teufelsmauer and the SCB is given in Klimczak (2011) and the electronic supplementary material.

Electronic supplementary material The online version of this article (doi:10.1007/s00531-012-0794-z) contains supplementary material, which is available to authorized users.

C. Klimczak (✉)
Department of Terrestrial Magnetism,
Carnegie Institution of Washington,
5241 Broad Branch Road, N.W.,
Washington, DC 20015-1305, USA
e-mail: cklimczak@ciw.edu

R. A. Schultz
ConocoPhillips, Geological Technology, PR2010,
600 North Dairy Ashford, Houston, TX 77079, USA

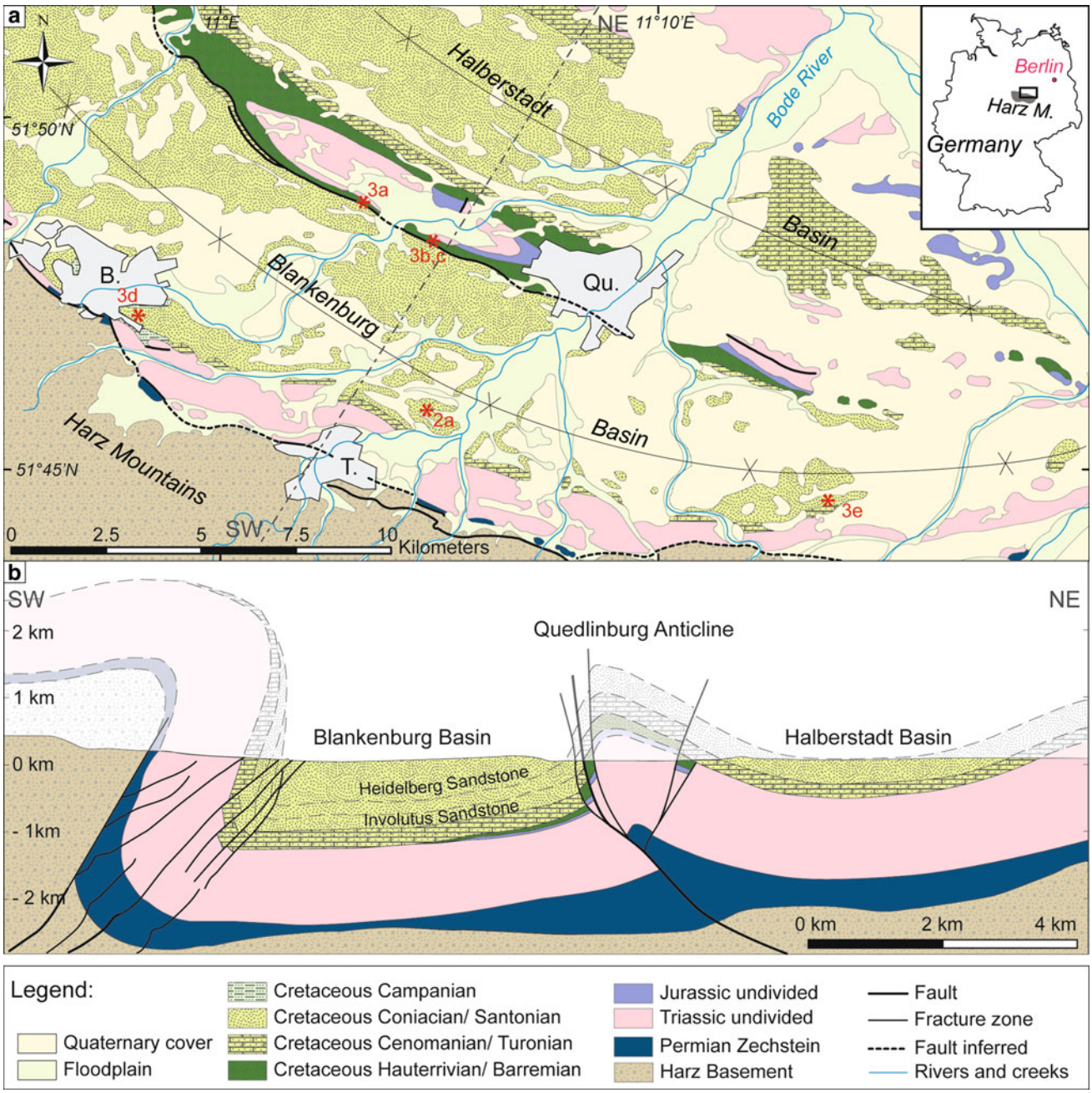

Fig. 1 Geology of the Subhercynian Cretaceous Basin, central Germany. **a** Simplified geologic and structural map of the Subhercynian Cretaceous Basin, central Germany (modified after Hinze et al. 1998). Towns in *gray*. *Qu* Quedlinburg, *B* Blankenburg, *T* Thale. Location of photographs and thin section pictures marked with *red asterisks*. **b** Geologic cross section from SW to NE based on core data, modified after Patzelt (2003) and Franzke et al. (2004), outlining the asymmetric nature of the Subhercynian Cretaceous Basin with its two sub-basins and interpreted folding above present day topography

Fault damage zones in porous rock

Pre-faulting strain localization in porous sandstone of upper crustal tectonic regimes is commonly found as deformation band damage zones. These damage zones contain dense populations of interconnected deformation bands, wherein each individual band reduces the porosity and increases the strain hardening properties of the host rock, which then facilitates the formation and propagation of a distinct large-displacement fault surface (e.g. Schultz and Siddharthan 2005; Aydin and Berryman 2010). They also commonly form barriers, baffles (e.g. Fossen et al. 2007) or conduits (Du Bernard et al. 2002a) for fluids and hence play a major role for fluid flow and fluid storage in

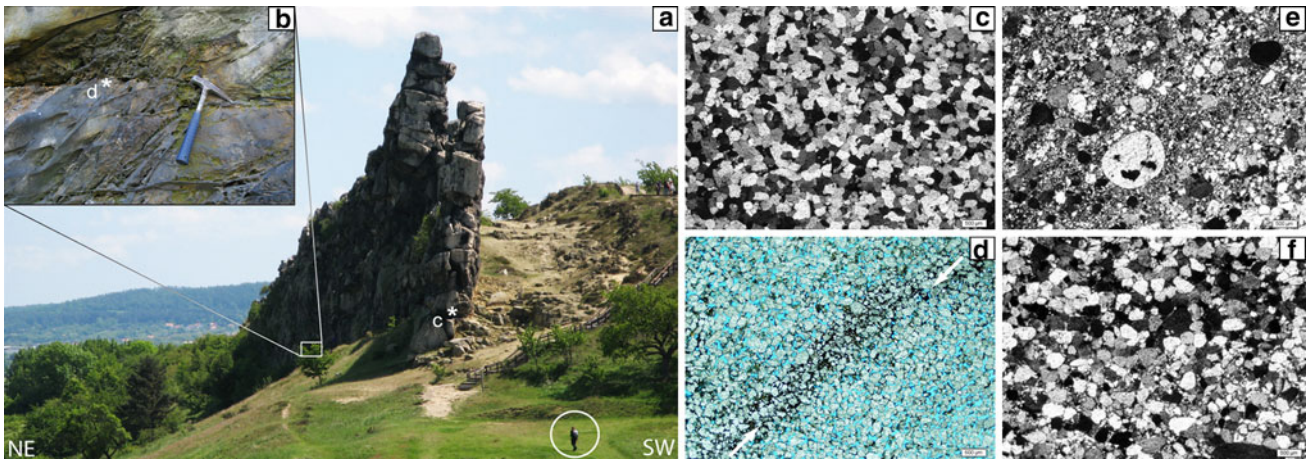

Fig. 2 The sandstones of the Teufelsmauer towers are deformed by several micro-mechanisms. **a** Prominent tower of the Teufelsmauer, at which the hardest rocks are heavily cemented sandstones—also frequently referred to as quartzite. Note person (*circled*) for scale. **b** Deformation bands in iron oxide and clay-rich beds bounding the heavily cemented horizon. **c** Cross-polarized photomicrograph of the *Heidelberg Sandstone* showing the crystalline texture of the highly cemented sandstones. **d** Plane-polarized photomicrograph of iron oxide and clay-rich sandstone with a deformation band. Note the smaller quartz grains and accumulation of iron oxides (*black*) in the band (*white arrows*). **e** Cross-polarized photomicrograph of typical cataclasis and cataclastic flow within the *Involutus Sandstone*. **f** Cross-polarized photomicrograph of the *Heidelberg Sandstone* showing dissolution transfer and cementation texture and minor cataclasis

porous rocks (Fossen and Bale 2007). Therefore, knowledge about deformation bands is important for petroleum and groundwater exploration and extraction as well as for relating deformation to fluid flow during the early stages of faulting in sedimentary sequences.

Fault-induced porosity reduction in sandstones can be achieved by several physical and chemical processes including mechanical compaction by reorganization of quartz grains, mechanical grain size reduction, and dissolution and cementation of quartz. These mechanisms lead to the formation of different types of deformation bands that can display similar macroscopic properties. Grain reorganization, often facilitated by iron oxide grain coatings (e.g. Underhill and Woodcock 1987; Main et al. 2001) and referred to as granular or particulate flow (Rawlin and Goodwin 2003; Twiss and Moores 2007), produces disaggregation bands. The reorganization can result in an initial porosity increase (e.g. Antonellini and Pollard 1995; Lothe et al. 2002; Du Bernard et al. 2002a) so that these types of deformation bands may also show some dilation. Mechanical grain size reduction, referred to as cataclasis (e.g. Engelder 1974; Passchier and Trouw 2005), causes cataclastic bands to form. Quartz dissolution, often catalyzed by the presence of chlorite, mica or clay minerals (e.g. Heald 1955; Houseknecht 1988; Oelkers et al. 1996; Renard et al. 1997), and subsequent cementation, often facilitated by the lack of these catalyzing minerals, lead to the formation of solution and cementation bands (Fossen et al. 2007; Torabi and Fossen 2009).

Fault damage zones in porous rock can display several localized or distributed deformation band network geometries including conjugate sets (e.g. Olsson et al. 2004; Saillet and Wibberley 2010) or ladder structures that resemble Riedel shear sets (e.g. Davis 1999; Davis et al. 2000). Typical ladders consist of a pair of parallel bounding deformation bands that are connected by antithetic linking deformation bands. The linking bands form as a response to stress interaction in the stepover region between the bounding bands (Schultz and Balasko 2003; Okubo and Schultz 2006). Ladders represent a progressive stage of deformation band damage zone development, where deformation is distributed in a tabular zone in which the rocks are strain hardened. Further strain then increases band thickness and eventually promotes localized deformation in the form of discrete planar slip surfaces (e.g. Shipton and Cowie 2001) that coalesce and ultimately result in through-going faulting (Schultz and Siddharthan 2005; Aydin and Berryman 2010).

While bands in damage zones from extensional tectonic settings tend to localize and cluster in narrow zones surrounding discrete fault planes (e.g. Johnson 1995; Davis 1999; Du Bernard et al. 2002b; Shipton et al. 2002; Saillet and Wibberley 2010), deformation band damage zones developing in compressional tectonic settings can form as distributed sets of conjugate or sequential bands as well as distributed arrays of ladder structures (e.g., Davis 1999; Klimczak et al. 2011). Such damage zones are characterized by systematic development of a vast number of

deformation bands in a widespread, evenly distributed, and pervasive manner throughout entire layers as observed in the Navajo Sandstone of the Colorado Plateau, USA, associated with the Rubys Inn thrust (Davis 1999) or in sandstones of the Orange quarry in the *Bassin du Sud-Est*, France, associated with Pyrenean shortening (Saillet and Wibberley 2010; Klimczak et al. 2011).

The above-described deformation band damage zone characteristics, that is, fracturing mechanisms responsible for porosity reduction, band geometries and distribution of bands in systematic networks, are all found associated with the fractures in the segments of the Teufelsmauer. Therefore, we conducted a field study to investigate whether these previously reported fractures are, indeed, deformation bands that are part of one or several deformation band damage zones. In order to accomplish this, we document the geometries and microstructural characteristics of the fractured and deformed sandstones, map the distribution and intensity of the deformation in the sandstones in relation to the location of the segments of the Teufelsmauer, as well as analyze the kinematics expressed by the fractures. These data are then related to the overall geometry and structural style of the Harz border fault.

Deformation bands in the SCB

The individual segments of the Teufelsmauer are found in the units of the *Neocomian*, *Involutus* and *Heidelberg Sandstones*, and consist of mostly white and some dark yellow or brown, well-sorted, highly porous, consolidated sandstones. The degree of sandstone consolidation is mainly governed by the fractures pervading the sandstones (Fig. 2b). These fractures, ranging in thickness from a few millimeters up to a few decimeters, are more resistant to weathering than their host rock. They weather out in positive relief and show a finer grained texture than the surrounding rock. Thicker fractures (>5 cm) display a cryptocrystalline, massive quartz texture. These observations agree with those made by earlier studies (e.g., Stackebrandt and Franzke 1985; Stackebrandt 1986; Franzke 1990; Patzelt 2003). Sandstones in the SCB displaying this massive quartz texture are often referred to as "quartzite" in the German literature. A discussion of the applicability of this term is included in the online supplementary material.

Microscopic inspection of these fractures reveals that they display a significant amount of porosity reduction across them. Host rock porosities of ~15–20 % are reduced to as low as 10–1 %, depending on the micromechanism causing the porosity decrease (Fig. 2c–f). Cataclasis occurs most abundantly (Fig. 2e) and is found throughout all three stratigraphic units associated with the Teufelsmauer. In addition, particulate flow (Fig. 2d), dissolution (Fig. 2f), and cementation (Fig. 2c) occur in the Teufelsmauer segments of the *Heidelberg Sandstone*. Particulate flow is also observed to cause a volume increase in some fractures, so that iron oxide and clay minerals can accumulate there (Fig. 2d). The observed mechanisms in the fractured parts of the sandstones of the SCB are consistent with mechanisms associated with the formation of deformation bands. Therefore, we interpret the fractures in the Teufelsmauer segments as deformation bands. Due to the involvement of different deformation mechanisms, cataclastic, disaggregation, and dissolution and cementation bands are observed in the SCB. A characterization of the microtextural and compositional properties of the sandstones and elucidating the role of iron oxide and clay coatings on the deformation of the quartz grains is presented in section "Microstructural characterization deformation band bearing sandstones" of this paper.

The fracturing, that is, deformation band formation, hardened the sandstones along the deformed zones. Hardening of the cataclastic bands is accomplished by the increased grain angularity leading to grain interlocking (Fossen et al. 2007), while dissolution and cementing in solution bands as well as accumulation of iron oxides in disaggregation bands welded the sandstones together, making them more resistant to weathering. Therefore, the development of deformation bands in the sandstones is responsible for their consolidation and, hence, for the prominent positive relief of most of the sandstone towers of the Teufelsmauer. The dependence of sandstone consolidation on deformation bands is supported by the presence of unconsolidated, soft host rock in the intervening zones between the bands, similar to its flat lying, undeformed equivalent in the center of the Blankenburg Basin.

Further evidence for a widespread network of deformation bands is found in the occurrence of ladder structures. Ladder structures with "backward-breaking" linking band angles are diagnostic of deformation band arrays (e.g. Schultz and Balasko 2003). We identify ladder structures (Fig. 3a) as well as conjugate sets of bands (Fig. 3b, c). They are developed in a similar manner to the ladder structures observed in Utah (Davis 1999; Davis et al. 2000) and the bands observed in the Orange quarry, France (Wibberley et al. 2000; Saillet and Wibberley 2010; Klimczak et al. 2011). The bands pervade the layers in which they grow in a systematic manner, distributed in wide deformation zones with different deformation band intensities. The large number of bands (Fig. 3c–e) with very narrow spacing (Fig. 3a, c) and the thickness of some bands (Fig. 3d) are particularly remarkable.

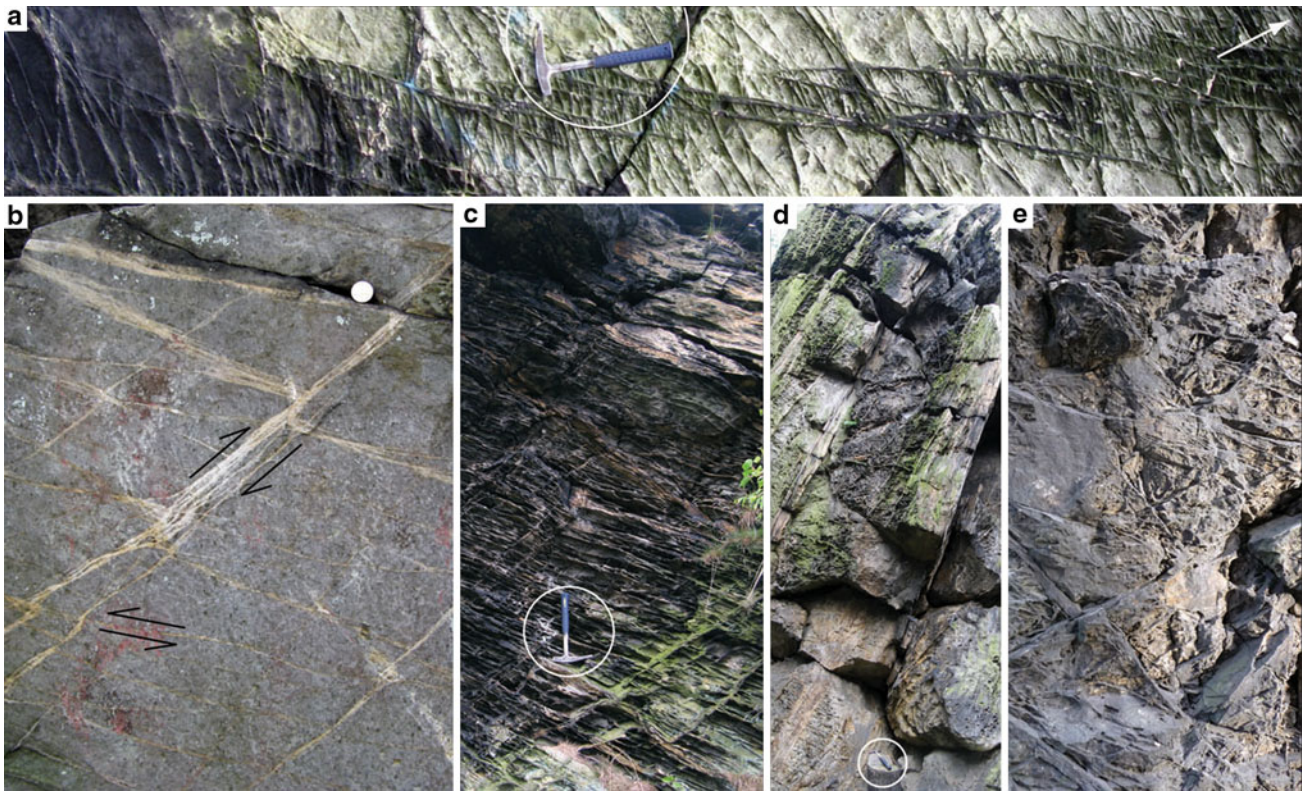

Fig. 3 Deformation band network patterns found in the SCB. **a** Array of deformation bands displaying ladder structures in the *Neocomian Sandstone*. Photograph is rotated, up is indicated by *white arrow*. **b** Conjugate bands in the *Involutus Sandstone* with thrust-sense kinematics indicated by *black half-arrows*. Note Euro coin for scale, up is to the *top* of the photograph. **c** Densely spaced conjugate bands in the *Neocomian Sandstone*. Toward the top of the picture bands become so densely spaced that rock appears quartzitic. **d** Deformation band network consisting in the *Heidelberg Sandstone* with very thick individual bands and several ladder arrays. **e** Disorganized deformation band pattern in the *Involutus Sandstone*. Note hammers (*circled*) for scale in parts **a**, **c**, and **d**

Development of deformation bands in different sandstone layers

The deformation band–bearing parts of the *Neocomian Sandstone* are mainly colored beige to white and are well sorted with grain sizes of 300–500 μm, but in places up to 700–1,000 μm. In this unit, deformation band geometries are well organized and display textbook ladder geometries (Fig. 3a). Up to 150-m-thick (Patzelt 2003) *Involutus Sandstone* crops out at both flanks of the Blankenburg Basin; however, deformation bands only occur in a ~10–20 m horizon in the southeastern part of the basin (Fig. 4). There, the sandstone is of white to beige color, but along the deformation bands, it can be discolored yellowish brown to dark red. Within this part of the *Involutus Sandstone*, grains are poorly sorted with sizes ranging from 250 up to 1,000 μm. Deformation bands pervade the sandstone, however, in a more or less disorganized pattern (Fig. 3e), where ladder geometries are not apparent.

The *Heidelberg Sandstone* is usually very clean, evident by its pure white color, but clay lenses and horizons as well as iron oxides can locally lead to yellow to brown and rusty discolorations. Grain sizes within this unit vary from 250 up to 1,000 μm, where individual horizons contain well-sorted sandstones whereas other horizons consist of poorly sorted rocks. Therefore, associated deformation bands exhibit the entire range of patterns as described above, depending on the grain properties of the sandstone.

As part of the *Heidelberg Sandstone* unit, a zone of highly cemented sandstone occurs, that weathers out as up to 30 m high towers (Fig. 2a). Voigt and von Eynatten (2004) document that the cementation filled up to 90 % of the pore space. This layer is up to 5 m thick and developed as either a single thick layer or as two separate thinner (1–2 m) layers, divided by a 5-m thick clay-rich layer. These rock towers also contain deformation bands, but they are overprinted by the cementation, and thus, they do not weather out as prominently as in the less quartz-cemented parts of this unit.

On the outcrop scale, observations show that sorting, grain size and initial porosity of the sandstones influence the deformation band geometries. Well-sorted sandstones with a high initial porosity display well-organized deformation band geometries, including well-developed ladder structures (Fig. 3a) and parallel, equally spaced bands (Fig. 3a, c). Sandstones with a lower porosity but good sorting show ladder structures as well. However, these

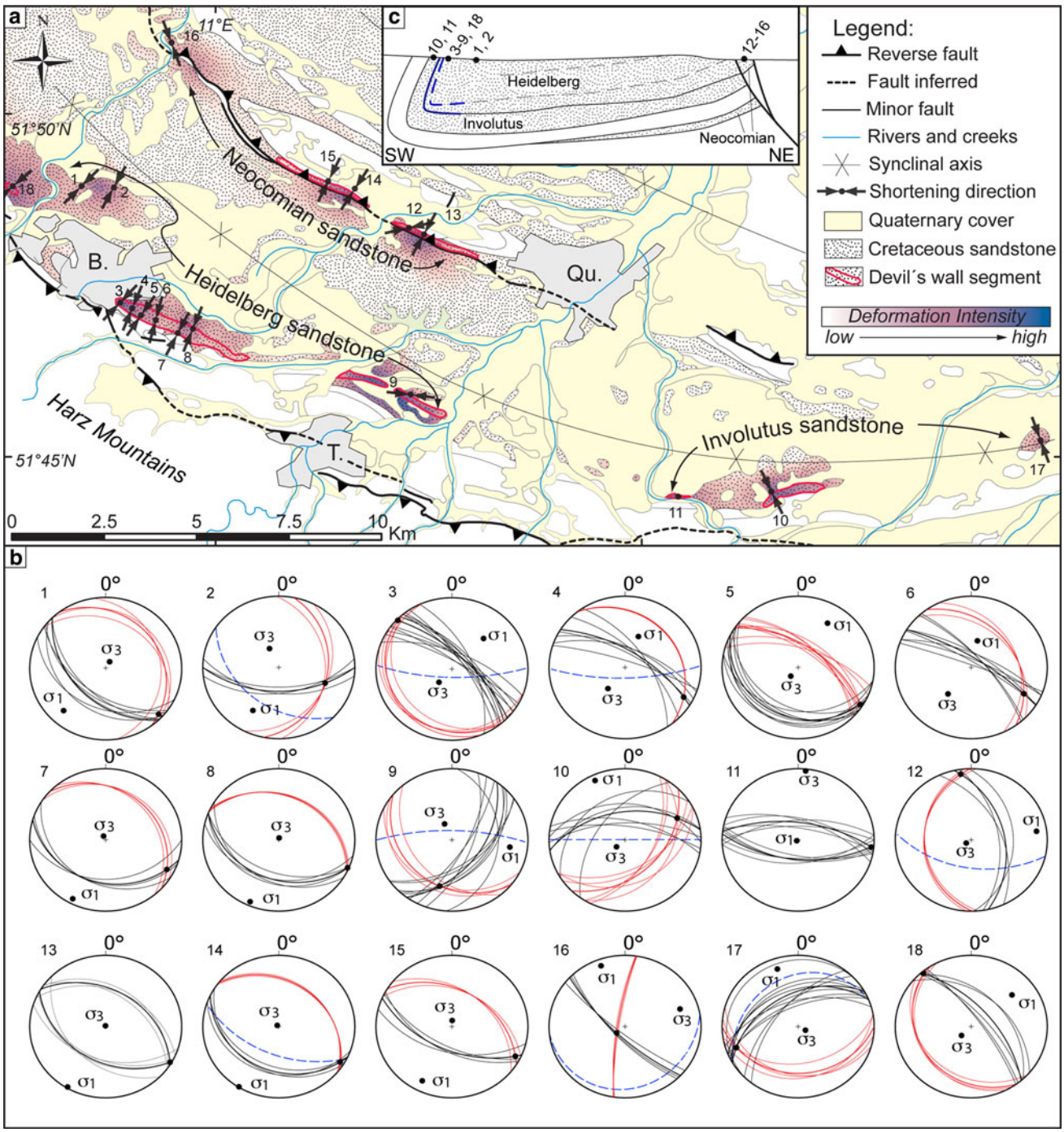

Fig. 4 Strain intensity and kinematics recorded by the bands. **a** Intensity map of the Cretaceous sandstone in relation to the segments of the Teufelsmauer, the stratigraphic units (*Neocomian, Involutus* and *Heidelberg Sandstones*), and the shortening directions of 18 representative stations. Note the rotation of shortening direction with the curvature of the synclinal axis of the Blankenburg Basin. **b** *Lower hemisphere* equal area representations of the bands with constructed axes of maximum and minimum compression. Bounding bands are shown in *red*, linking bands as well as conjugate sets of bands are shown in *black*, and bedding is plotted in *blue*. The majority of bands are developed synthetically or antithetically to the Harz border fault. **c** Simplified cross section from SW to NE based on Fig. 1b. Measurement localities are shown with respect to the fold structure and approximate locations of unconformities (*blue lines*)

ladders are not as systematically organized, linking bands are not parallel to each other, and the spacing of the bands is unevenly distributed (Fig. 3d). Poorly sorted sandstones do not develop ladder structures; instead, bands are organized in conjugate or chaotic arrays (Fig. 3e). Based on these field observations, it can be inferred that physical properties of the sandstones influence the deformation band geometries.

Microstructural characterization deformation band–bearing sandstones

The different parts of the deformation band damage zone in the SCB are deformed by different micro-mechanisms, that is, cataclasis, particulate flow and dissolution transfer and cementation (Fig. 2c–e). Optical microscopy reveals that the deformation bands contained in the *Neocomian* and *Involutus Sandstones* are predominantly formed by cataclasis (Fig. 2e). The *Heidelberg Sandstone* is locally affected by cataclasis; however, the majority of it is deformed by several other mechanisms including particulate flow, dissolution transfer and quartz cementation, resulting in disaggregation bands (Fig. 2d), solution bands (Fig. 2f) and quartz cementation (Fig. 5b), respectively.

Grain fracturing and crushing occurs in all three deformation band bearing units of the SCB; however, typical cataclastic bands are only found in the *Neocomian* and *Involutus Sandstones*. Thick bands and wide deformation zones in these sandstones (e.g. Fig. 3c) are affected by cataclastic flow, where crushed grains form a fine matrix around large, well-rounded, undeformed grains (Fig. 2e). This finding was similarly described by Tiwari and Roy (1974) also from the *Involutus Sandstone*, where they reported fractured and unfractured quartz clasts within a predominantly fine-grained quartz matrix, to which they referred to as "silicified."

The majority of grains within the cataclastically deformed *Neocomian* and *Involutus Sandstone*s are devoid of any clay or iron oxide coatings. This is consistent with studies that found that the lack of such coatings promotes fracturing of the grains and ultimately cataclasis, since friction between individual grains inhibits sliding along grain boundaries (Underhill and Woodcock 1987; Main et al. 2001). Furthermore, cataclastic deformation mechanisms are favored with higher grain contact stresses (e.g. Flodin et al. 2003), which can be achieved with higher porosities and larger grains. Within the *Neocomian* and *Involutus Sandstones*, the grain size tends to be greater than in the *Heidelberg Sandstone*, supporting the tendency for cataclastic deformation in these units.

Disaggregation bands develop from shear-related disaggregation of grains (e.g. Fossen et al. 2007) where neither significant grain fracturing nor dissolution occurs. The disaggregation bands in the SCB are found in the less intensely deformed parts of the *Heidelberg Sandstone*. These parts of the sandstone are less consolidated and poorly lithified, which are preferred properties for the formation of disaggregation bands (Mandl et al. 1977; Du Bernard et al. 2002a; Bense et al. 2003). Dislocation and slight rotation of grains compacted and either reduced or even increased the porosity of the sandstone slightly (Fig. 2d). This change in porosity is indicated by an accumulation of clay and iron minerals in or along the disaggregation band (Fig. 2d, black material in the band). As opposed to the *Neocomian* and *Involutus Sandstones*, iron oxide and clay minerals are found abundantly as grain coating or lining, pore filling, and where fractured grains occur also as fracture filling (Fig. 5a–c). Pore filling by iron minerals is mostly compact (Fig. 5a, black arrow) whereas clay minerals are abundantly found as vermicular or filamentary pore filling structures (Fig. 5a, white arrow). Opposite to the lack of iron oxide grain coatings, their abundant occurrence along or in the bands, as evident from optical (Fig. 5a) and energy dispersive X-ray spectroscopy (EDS) mapping (Fig. 5b), reduces the friction between contacting grains and therefore promote sliding along grain boundaries (Underhill and Woodcock 1987; Main et al. 2001; Torabi and Fossen 2009). Thus, the formation of disaggregation bands was likely favored over cataclasis in these parts of the *Heidelberg Sandstone*.

Solution bands in the SCB appear similar to disaggregation bands, but dislocation and rotation of grains compacted and reduced the porosity of the sandstone more than for the disaggregation bands. The majority of the detrital grains are coated with clay and iron minerals (Fig. 5c), so that grain crushing is inhibited. The presence of clay mineral grain coatings, evident from optical microscopy (Fig. 5c) and element mapping (Fig. 5d), promotes the dissolution of quartz (e.g. Heald 1955; Houseknecht 1988; Oelkers et al. 1996; Renard et al. 1997), welding detrital grains together with straight overgrowth faces and triple junctions with 120° angles (Fig. 5c, black arrows). Furthermore, precipitation and cementation of dissolved quartz is inhibited where clay and iron oxide minerals coat the majority of grains (e.g. Füchtbauer 1967b; Pittman 1972; Heald and Larese 1974; McBride 1989). These findings are in accord with the results of Franzke (1990), where a densely fractured part of the *Heidelberg Sandstone* was sampled and analyzed by optical, scanning electron, and cathodoluminescence microscopies. There it was found that fractured parts of the sandstone show dissolution transfer, cataclasis and cementation in pore space between fractured grains, whereas undeformed parts of the porous (>20 %) sandstone are mostly devoid of these characteristics.

As compared to the texture within a thick cataclastic band (Fig. 2e), a thick dissolution band shows less of a fine-grained matrix and higher proportion of larger sized grains (Fig. 2f) with different dissolution grain-to-grain contacts. The majority of contacts are truncating grain contacts, which are flat or slightly curvy grain interfaces (Fig. 5e) that occur due to the equigranular nature of the sandstones. Mostly similar sized grains with similar radii contact each other. In places, indenting grain contacts between two unequally sized grains occur, where the smaller grain indents the larger one. Due to the high amount of catalytic minerals present in some parts of the

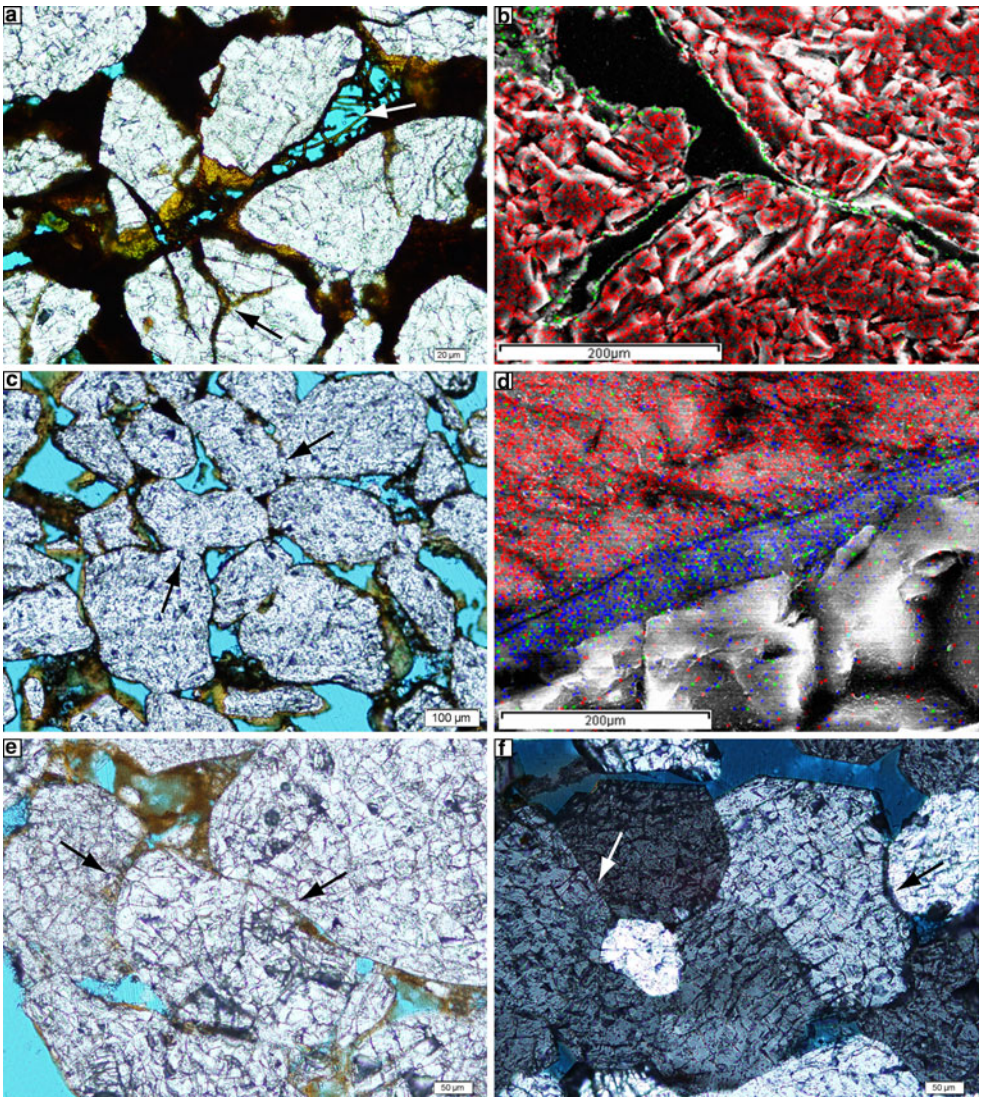

Fig. 5 Microstructural characteristics of the *Heidelberg Sandstone*. **a** Plain polarized photomicrograph of the pore filling with clay and iron oxide minerals developed as massive pore filling, grain coating, fracture infill (*black arrow*) and vermicular structures (*white arrow*). **b** EDS Element map of quartz grains (silica mapped in *red*) thinly coated with iron oxides (iron mapped in *green*). **c** Plain polarized photomicrograph of coated detrital grains of less compacted sandstone showing dissolution transfer (*black arrows*). **d** EDS Element map of the clay grain coating surrounding a quartz grain (*gray*) indicated by iron (*green*) and aluminum (*blue*) adjacent to anhydrite pore filling (calcium mapped in *red*). **e** Plain polarized photomicrograph of slightly curvy dissolution transfer truncating grain contacts. **f** Cross-polarized photomicrograph of the cemented sandstone showing quartz overgrowths with typical straight crystal contacts (*white arrow*) and 120° crystal boundary triple junctions but also indented grain boundaries indicating dissolution transfer (*black arrow*)

Heidelberg Sandstone, dissolution is accelerated, resulting in very thick solution bands.

The prevalence of catalytic minerals in the *Heidelberg Sandstone* inhibits the cementation of quartz (Füchtbauer 1967b; Pittman 1972; Heald and Larese 1974; McBride 1989); however, the most prominent part of the *Heidelberg Sandstone* is characterized by a pervasive heavy cementation (Fig. 2c), making it stand out so prominently from the lesser-cemented rock layers, surrounding it (Fig. 2a). The grains within this particular horizon are very clean, and they are devoid of clay coatings and iron oxides are rare. *Heidelberg Sandstone* sections analyzed by Tiwari and Roy (1974) already revealed some layers with quartz grains in a clay matrix while other compacted parts of the sandstone were without clay but showed a heavy cementation, with the individual grains held together by autigenic quartz. Voigt and Eynatten (2004, 2006) showed that cathodoluminescent detrital quartz grains are overgrown by thick non-luminescent quartz cement, where the cement is in optical continuity with the grain.

Quartz overgrowths are selective to beds of a particular grain size, where the majority of studies document a preference of overgrowths for finer grained sandstones (Heald and Renton 1966; Füchtbauer 1967a; Stephan 1970; McBride 1989; Dewers and Hajash 1995). Moreover, quartz arenites are best suited to form quartz overgrowths (McBride 1989), with those also more likely to form well-developed patterns, such as straight overgrowth faces and triple junctions with 120° angles, when the detrital grains are monocrystalline (James et al. 1986; McBride 1989). The heavily cemented beds of the *Heidelberg Sandstone* mostly lack thick mineral coatings (Fig. 5f) are relatively fine-grained quartz arenites and are composed of monocrystalline quartz grains (Figs. 2c, 5f), favoring quartz overgrowths as the predominant cementation mechanism in these parts of the sandstone.

Deformation band damage zone origin of the Teufelsmauer

Kinematics of the deformation bands

Band orientations were measured at all segments of the Teufelsmauer. Comparison of band orientations from the different segments of the Teufelsmauer can highlight whether the bands are kinematically and genetically linked to each other and potentially to the Harz border fault. Furthermore, angular relationships of conjugate bands or linking and bounding bands of ladder structures allow the determination of the principal stress axes and, hence, provide insights into the local and regional stress fields. This will show whether the stress axes are consistent with the general Cretaceous tectonic activity in the area.

The vast majority of the fractures in the SCB are developed as reverse-sense deformation bands, evident from linking- and bounding band arrangements in ladder structures (Okubo and Schultz 2006; Fig. 3a) as well as offsets of sedimentary laminations and mutual offsets of conjugate band arrays (Fig. 3b). A very few localities show bands accommodating normal or strike-slip kinematics.

Deformation band orientations were measured at over 30 stations throughout the eastern SCB, and data from 18 representative stations are shown in a map and as lower hemisphere equal area plots (Fig. 4a, b). Orientations at most stations show two sets of bands of ladder structures, where the bounding bands are marked in red and linking bands are marked in black, or conjugate sets, where both sets are shown in black. Bedding orientation is plotted in blue. The orientations of the bands of the individual stations are fairly consistent with each other throughout the SCB. Many of the bands have a strike of NW–SE, consistent with the local trends of the Harz border fault and associated nearby faults and the fold axis of the Blankenburg Basin (Fig. 4a, b). As a side effect of the faulting and folding being related (e.g. Voigt et al. 2004), deformation bands frequently show similar strikes to the overall bedding in the area. However, no systematic relationship is apparent from comparison of band dips with bedding attitudes (Fig. 4b), with respect to the unconformities and layer rotation (Fig. 4c).

With respect to the Harz border fault, the NW–SE striking bands are either developed synthetically, that is, bands dip in the same direction as the fault, or antithetically, that is, bands have opposite dip directions with regard to the fault. In 15 of the 18 shown stereonet plots (Fig. 4b), there are bands with at least one set, if not both, that are developed in such a synthetic or antithetic manner to the Harz border fault. These 15 stations are located throughout all segments of the Teufelsmauer. This shows that deformation band orientations at individual stations are generally consistent with the overall orientation of the Harz border fault in all parts of Teufelsmauer and therefore suggests that these bands are all part of one deformation band damage zone.

Based on the bimodal nature of the antithetic and synthetic bands (Fig. 4b), that is, forming preferably as one set of orientations of ladders or conjugate bands rather than polymodal patterns (Healy et al. 2006), we determined the orientations of principal stress axes considering the classical Mohr-Coulomb failure criterion (e.g. Marshak and Mitra 1988; Johnson 1995), where the orientation of the axis of maximum compression (σ_1) coincides with the acute bisector between the two sets of deformation bands (Fig. 4b). The orientation of the axis of maximum compression corresponds to the axis of maximum shortening (e.g. Twiss and Moores 2007). This information was then used to display the orientation of the shortening direction in map view (Fig. 4a) by projecting the σ_1 axis to horizontal along the vertical plane it is contained in. The 18 resultant shortening directions are plotted in Fig. 4a.

By relating these shortening directions to the observed strain geometries in the SCB, we find that shortening directions from deformation bands generally trend NE–SW, perpendicular to the fold axis of the Blankenburg Basin and the trace of the Harz border fault (Fig. 4a). This is consistent with the overall NE–SW shortening direction of the Harz border fault and the folding of the SCB (e.g. Franzke and Schmidt 1995; Franzke et al. 2004). Shortening directions also mimic local variations of the strike of the fault. The change of orientation from an NW–SE to an E–W strike of the Harz border fault and the Blankenburg Basin fold axis in the SE of the SCB (Figs. 1a, 4a) is also reflected in the rotation of shortening directions in that area (Fig. 4, stations 10 and 17). The consistency of shortening directions from the bands with the overall tectonic

shortening direction expressed by the faulting and folding shows again that the deformation bands of all segments of Teufelsmauer are likely to have developed as one coherent damage zone associated with the Harz border fault.

The total of our band orientation measurements of $n = 273$ is presented as a density plot in relation to the average Harz border fault orientation (e.g. Stackebrandt 1986; Franzke et al. 2004) in a lower hemisphere equal area stereonet, where the darker areas indicate a higher density of poles to measured band orientations (Fig. 6a). The stereo plot shows two maxima of densities of poles to the bands in the NE and SW quadrants. The maximum of band orientations in the NE quadrant of the plot coincides with the average orientation of the Harz border fault (Fig. 6a), while the maximum of band orientations in the SW quadrant of the plot represents all antithetic bands. This match in band and fault orientations confirms that (1) the majority of deformation bands are consistent with the orientation of the Harz border fault by having developed either synthetically or antithetically to it and (2) that there was no more significant tilting of the layers after the deformation bands had formed.

The 18 orientations of the axes of maximum (σ_1) and minimum compression (σ_3) are compiled in a lower hemisphere equal area plot (Fig. 6b) in relation to their average values, a value for σ_1 obtained from fractures in the area by Stackebrand and Franzke (1989), and the average orientation of 110/35 SE (Fig. 1) of the interpreted fracture zone (Franzke et al. 2004) as a trajectory to the deep structure of the Harz border fault (Fig. 1b). The average values for σ_1 are oriented horizontally close to the value from the literature. Both values are consistent with a NE–SW shortening of the area and also match the stress analysis by Franzke and Schmidt (1995) for reverse-sense fractures near our station 9 in Fig. 4. The shortening direction at station 9 in our analysis shows a deviation from the overall NE–SW shortening. Nearby, König and Wrede (1994) present evidence for strike-slip kinematics of the Harz border fault. Despite the deviation of shortening direction, we do not confirm a strike-slip motion of the bands. The bands display a thrust sense, evident from the kinematics of present ladder structures with relatively shallowly dipping bounding bands.

Additionally, the horizontal orientation of σ_1 and vertical orientation of σ_3 for both average values of principal stress axes (Fig. 6b) and at most individual stations (Figs. 4b, 6b) are consistent with thrusting (e.g. Anderson 1942; Johnson 1995). When comparing the angular relationship of the obtained principal stresses from the bands to the average orientation of the Harz border fault fracture zone as inferred by Franzke et al. (2004), we find that σ_1 and σ_3 are inclined by $\sim 35°$ and $\sim 55°$ to the fault, respectively (Fig. 6b). These angles also agree well with

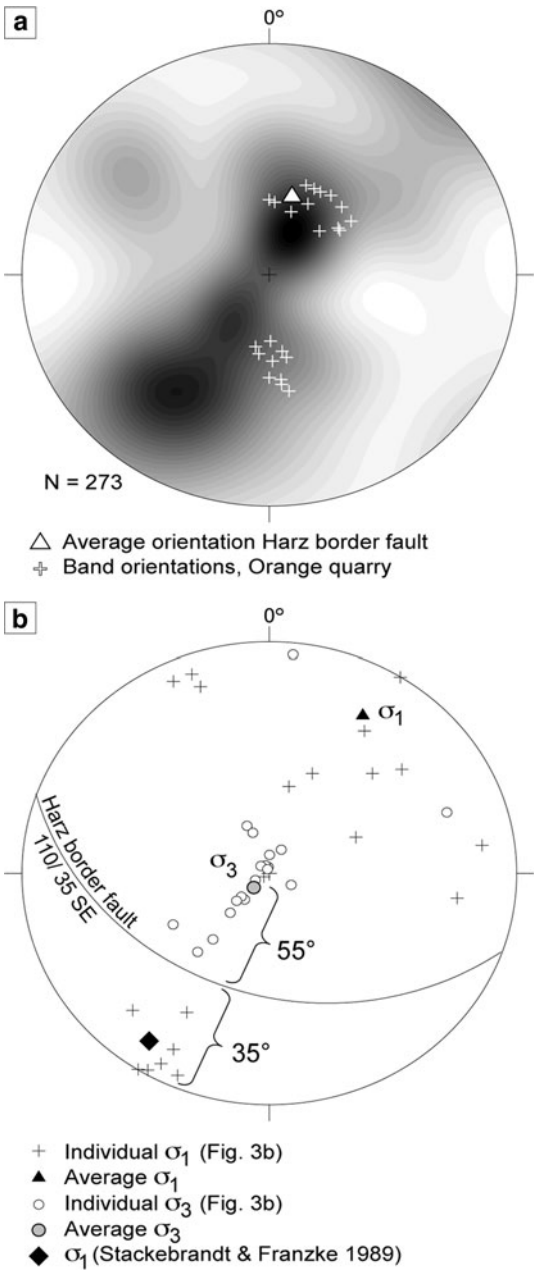

Fig. 6 *Lower hemisphere* equal area plots of band orientations and principal stress axes. **a** Density plot of poles of 273 band orientations. Higher densities of orientations are contoured with darker colors. There are two maxima of orientations in the NE and SW quadrant. Band orientation maximum in the NE quadrant coincides with the average orientation of the Harz border fault. Density of deformation bands of the SCB is shown in relation to bands from the Orange quarry, Bassin du Sud-Est, France (Klimczak et al. 2011). **b** Compilation of axes of minimum and maximum compression from Fig. 3b relative to average orientation of the Harz border fault. Average values of minimum and maximum compression plot *horizontally and vertically*, respectively. Average maximum compression plots close to the value from the literature (Stackebrand and Franzke 1989)

the theoretical angles of 30° and 60° of maximum and minimum compression to thrust faults (Anderson 1942). This kinematic analysis demonstrates a consistent sense of

thrusting of deformation bands throughout all segments of the Teufelsmauer that is also compatible with the kinematics of the Harz border fault. It further underlines the role of the deformation bands of the Teufelsmauer as a coherent damage zone that is genetically linked to the Harz border fault.

Strain intensity

We evaluated the intensity of deformation band development at all segments of the Teufelsmauer in order to gain insights into the distribution of sandstone deformation throughout the eastern SCB. This information can be used to define the geometry and geographic extent of the deformation band damage zone and is therefore helpful to characterize the spatial relation of the damage zone to the Harz border fault. Based on prior reports on different deformation zones associated with tilting of the layers along the Harz border fault (Stackebrandt 1983, 1986) and the degree of quartzitification or silification of the sandstones (Schulschenk 1930; Heimlich 1956), we have visually estimated the intensity of deformation band development at all segments of the Teufelsmauer and its surrounding rocks, as well as several outcrops throughout the eastern SCB. The intensity was categorized into five qualitative stages after a methodology by Riller and Schwerdtner (1997) and Klimczak et al. (2007), depending on thickness, density and interconnectedness of deformation bands. Stage zero in our analysis represents the undeformed rock leading up to stage five with progressively increasing band thicknesses and densities. The heavily cemented towers of the Teufelsmauer (Fig. 2a) are also assigned highest deformation intensities.

A strain intensity map (Fig. 4a) was geostatistically generated by interpolating between the stages of the visited field locations using the Kriging method. Kriging is a commonly used interpolation method in the geosciences (Matheron 1963), which predicts distance-weighted average values for locations where values were unknown, based on surrounding known values. Lower intensities are shown in light red, grading into a dark purple for very high deformation intensities.

This strain intensity distribution shows the large-scale geometric character of the deformation band damage zone, where two elongated narrow zones of higher intensities were identified parallel to the two main faults in the region. The two damage zones are located (1) within the layers of the *Neocomian Sandstone* to the North and (2) in the *Involutus* and *Heidelberg Sandstones* to the South (Fig. 4a). The northern damage zone completely surrounds a previously mapped fault. In particular, the maximum intensities coincide with the center of the fault. The southern deformation band damage zone runs some 100 m to at most a few kilometers northward of and subparallel to the Harz border fault. Here, the maximum deformation intensities seem to have no clear geographic correlation to the fault. They occur more or less equally distributed along the damage zone.

Since the northern portion of the damage zone displays the highest intensities at the center of the fault (Fig. 4a), where one would expect also the highest fault displacement, it is interpreted as a damage zone directly surrounding the fault plane. Deformation bands formed as precursors to the faulting, facilitating the development of a through-going fault plane. The damage zone in the southern part of the Blankenburg Basin seems not to be in direct contact with a fault. This behavior is common around fault tips, where the fault has not yet propagated into the surrounding porous rock, but deformation bands already formed as precursors of the fault in its tip region. The southern deformation band damage zone seems to either have formed in the tip region of the Harz border fault or else may represent the accompanying damage zone at the vicinity of it (Fig. 4a), where conditions were appropriate for deformation bands to develop but unfavorable in rocks directly surrounding the fault.

The northern damage zone occurs in a single lithology only, where properties are fairly homogenous along strike. Therefore, the controlling factor for the strain intensity appears to be the proximity and amount of offset along the fault. The southern damage zone is geographically closest to the Harz border fault, the largest tectonic structure in the area with a length of over 90 km and more than 3,000 m of stratigraphic offset (e.g. Stackebrandt 1983). The higher strain on the Northern Harz Mountains Border Fault may then have caused correspondingly higher deformation intensities over a much wider lateral extent, where effects on strain intensity from variations in offset and tectonic stresses along the fault are relatively minor. The formation and development of the laterally wider southern deformation band damage zone, which affects two lithologies, is therefore interpreted to be controlled by variations in rock properties.

From Fig. 4a it is apparent that the deformation band damage zone, as revealed by the strain intensity map, coincides with the extent of the segments of the Teufelsmauer. In particular, all rock towers of the Teufelsmauer contain a high concentration of deformation bands, pertaining to high deformation intensities. Due to the formation of the deformation bands and associated cementation, the highly deformed parts of the sandstones form the most weathering-resistant parts of the area and, hence, make the Teufelsmauer stand out so prominently (Fig. 2a).

Discussion

Implications for the tectonics affecting the SCB during the Late Cretaceous

The presence of a deformation band damage zone along the Harz border fault has important implications for its geometry and kinematics. A recent model re-interpreted the rotating unconformity pattern within the Upper Cretaceous rocks as the expression of a growing anticline above the thrusting Northern Harz Mountain Border Fault (Voigt et al. 2004; Fig. 1b). Although not mentioned in that paper, the sequence is also consistent with the growth of deformation band damage zones, as they frequently form in association with fault-related folds, when porous rocks are present within the folded layers. Prominent examples include deformation band damage zones in the East Kaibab Monocline, Utah, (e.g. Davis 1999) the Waterpocket fold, Utah, (e.g. Davis 1999; Katz et al. 2004) the San Rafael Monocline, Utah, (e.g. Davis 1999) and the Uncompahgre Fold, Colorado (Stearns and Jamison 1977; Okubo and Schultz 2005). Mapping of deformation band intensities in the Uncompahgre Fold (Jamison and Stearns 1982) and numerical modeling (Okubo and Schultz 2005) shows that a deformation band damage zone forms within porous, faulting-related folded layers above and along the fault. Band thickness and band interconnectedness are found in this study to have increased where the fault impinged upon the base of the porous layers, consistent with our findings for the SCB (Fig. 4a).

Our mapping suggests that the very thick and interconnected bands in the damage zone of the SCB formed above the tip of the Harz border fault (Fig. 1b). As evident from the intensity map (Fig. 4a), the southern damage zone associated with the Northern Harz Mountains Border Fault is not in direct contact with the main fault, but is separated by some hundreds to thousands of meters of evaporitic and limy Triassic and Upper Permian strata (Fig. 1b). As the fault impinged upon the sandstone layers, a damage zone representing the process zone at the fault tip and along the side of the Northern Harz Mountains Border Fault formed.

In the damage zone, deformation bands formed preferentially in a synthetic or antithetic manner to the Harz border fault (Fig. 6a). Orientations and angular relationship between synthetic and antithetic deformation bands permit a stress-field analysis that reveals thrust-sense kinematics of the bands in the damage zone (Figs. 4b, 6b), consistent with the overall thrusting character of the Harz border fault. This finding shows that the kinematics of the Harz border fault is reflected in the smaller-scale structures in the damage zone of the SCB. Therefore, further detailed analysis of the deformation bands and other closing-mode fractures, such as stylolites, in the damage zone would allow a detailed reconstruction of the overall stress-field as well as local stress-field variations.

The overall consistency of deformation band orientations with the average fault orientation in the vertically dipping layers (Fig. 6a) shows that bands formed at a late stage or after the tilt of the layers and that these layers did not experience much further rotation after the development of the bands. Since deformation bands are precursors to faulting and, hence, develop during the early stages of faulting, the observed consistency between band and fault orientations shows that the faulting affected the Cretaceous layers at an advanced stage of the folding of the SCB. In addition, the more or less uniform orientations of deformation bands throughout the deformed stratigraphic units, despite their progressive change of bedding (Fig. 4c) due to four major unconformities (Voigt et al. 2004), indicate that bands in all segments of the Teufelsmauer were formed contemporaneously along the entire Harz border fault system. This confines the timing of deformation band development between the youngest deformed layer, the *Heidelberg Sandstone* (~84 Ma), and the youngest unconformity, juxtaposing the vertically tilted *Heidelberg Sandstone* to near-horizontal, undeformed Campanian units (~83 Ma). Furthermore, the good agreement in shortening directions of deformation bands and Harz border fault indicates that the regional stress state did not change throughout the development of the Harz border fault in the late Cretaceous. The very few individual disagreements with overall kinematics and shortening directions (e.g. Fig. 4b, station 11) are here interpreted to local perturbations of the regional stress field.

Deformation bands have only been documented from a few continental settings in Europe, including bands in gravels in Austria (Exner and Grasemann 2010) and France (e.g. Wibberley et al. 2007; Saillet and Wibberley 2010; Klimczak et al. 2011). Several sets of cataclastic deformation bands at the *Bassin du Sud-Est* (BSE), Provence, France (Wibberley et al. 2007; Saillet and Wibberley 2010; Klimczak et al. 2011) occur in poorly consolidated, faulted Upper Cretaceous sandstones. Their tectonic origin is attributed to several phases of fault-related deformation, where the initial pulse of deformation resulted in thrust faulting that is related to North–South Pyrenean shortening (Wibberley et al. 2007; Saillet and Wibberley 2010). In terms of depositional environment of the sands, sandstone consolidation, tectonic setting, damage band network geometry, and band orientation (Fig. 6a), this deformation band damage zone shows striking similarities to our observations of bands in the SCB.

In particular, Cenomanian sandstones (~94 Ma) in the Orange quarry, BSE, display the same characteristics of a deformation band network, where thousands of deformation bands are evenly distributed throughout a single layer,

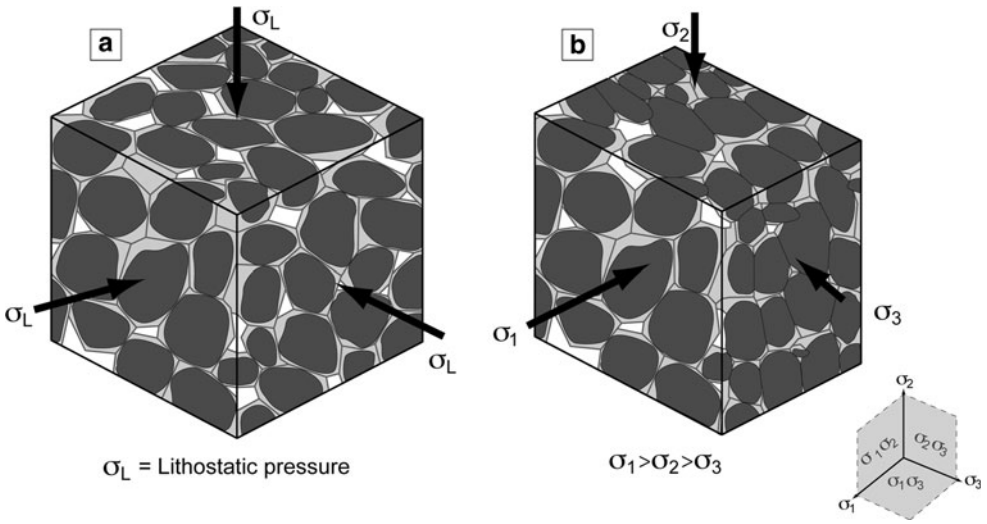

Fig. 7 Schematic comparison of isotropical to stress-induced quartz overgrowths. **a** Isotropic quartz overgrowths are directionally independent, and authigenic quartz grows equally in every direction. **b** Stress-induced overgrowths are directionally dependent, and overgrowths are preferred in the plane of minimum stresses ($\sigma_2\sigma_3$), where it does not differ from isotropic overgrowths. In the planes of maximum stresses ($\sigma_1\sigma_2$ and $\sigma_1\sigma_3$), overgrowths occur along with dissolution transfer

pervading the poorly consolidated sandstone. Here, the deformation band pattern, of which the origin is also attributed to thrust fault-related folding of the Cretaceous strata (Klimczak et al. 2011), is similarly developed to what we observe in the SCB. The Orange band network compares best to the conjugate sets of cataclastic deformation bands in the SCB of the *Neocomian* and *Involutus Sandstones* (e.g. Fig. 3b).

Origin of the sandstone cementation

The cementation in parts of the *Heidelberg Sandstone* was previously interpreted to have originated from fluid convective processes, such as migration of silica-enriched fluids from depth due to hydrothermal activity (Franzke et al. 2004), pore space infiltration driven by tectonic forces (Franzke et al. 2004, 2005) or groundwater hydraulic mechanisms (Voigt and von Eynatten 2004, 2006). Based on the observation that cementation is confined to the most porous rocks at both flanks of the basin, Voigt and Eynatten (2004, 2006) propose an idea where the cementation must have been due to artesian compaction waters that were driven by the load of ongoing sedimentation from the center of the basin to its flanks. Silica is assumed to originate from diagenetic alteration of feldspars to clays. It is argued that this process is likely because the cementation only appears at the flanks of the Blankenburg Basin in different stratigraphic units. However, there is no evidence for such convective processes and our microstructural investigation shows that the cementation only occurs at parts of the southern, vertically dipping flank of the basin, but all other quartzitic-appearing sandstones on both flanks of the basin are predominantly caused by cataclasis and pressure solution, processes clearly associated with sandstone deformation. Furthermore, the quartz overgrowths cemented horizons are located in the central portion of the deformation band damage zone (Fig. 4a, close to station 9), suggesting that tectonic processes associated with the Harz Mountains uplift influenced the quartz overgrowths cementation.

Blenkinsop (2000) presents two quartz overgrowth mechanisms, that is, isotropic overgrowths (Fig. 7a) and stress-induced overgrowths (Fig. 7b). While isotropic overgrowths arise from mutual impingement of overgrowing quartz, growing at equal rates in all directions from adjacent detrital grains, stress-induced overgrowths are directionally dependent, growing only in the direction of the least stresses. In this case, inter-granular dissolution transfer occurring in the plane of the maximum stresses channels the silica in the direction of the least stresses by diffusion. This mechanism has been successfully reproduced in compaction experiments (e.g. Renton et al. 1969; de Boer et al. 1977; Gratier and Guiget 1986; Schutjens 1991).

Since stress-induced overgrowths involve dissolution transfer and quartz overgrowths, microscopic analyses should reveal characteristics of both mechanisms. Indeed, microscopic inspection of the cemented parts of the *Heidelberg Sandstone* shows typical straight overgrowth faces (Fig. 5f, white arrow) and triple junctions with 120° angles but also thinly clay-coated grains indenting into neighboring quartz grains (Fig. 5f, black arrow). Due to the anisotropic nature of stress-induced quartz overgrowths, the dissolution transfer and overgrowths characteristics are differentially developed in the three dimensions (Fig. 7b). In the planes of the maximum stresses, silica is mainly dissolved, so that predominantly dissolution grain-to-grain contacts occur. Along these planes, silica can be precipitated perpendicular to σ_1 (Fig. 7b). In contrast, within the plane of minimum compression, almost no dissolution transfer occurs and silica is exclusively precipitated resulting in a typical overgrowth pattern. As a result, the

stress-induced overgrowth pattern in the plane of the minimum compression can look identical to isotropic overgrowths (Fig. 7a). By means of cathodoluminescence, Voigt and Eynatten (2004, 2006) determined that the cemented *Heidelberg Sandstone* was a relatively loosely packed sandstone, prior to the quartz overgrows, showing a rather isotropic pattern. If their thin sections were taken in the plane of the minimum compression (Fig. 7b), the observed isotropic overgrowths pattern would be indistinguishable from stress-induced quartz overgrowths. Combining all observations, the cementation of the *Heidelberg Sandstone* in the damage zone associated with the Harz Border Fault is consistent with stress-induced quartz overgrowths.

The occurrence of heavy cementation by the quartz overgrowths raises the question whether it was facilitated by deep burial or hot fluids migrating through the rock. However, there is no evidence for hydrothermal activity in the area (e.g. Voigt and von Eynatten 2006) nor was the *Heidelberg Sandstone* buried to great depths (Franzke et al. 2004), as evident by its very low degree of consolidation in the central parts of the Blankenburg syncline. The SCB is believed to have experienced subsidence from Albian to Turonian times, followed by an accelerated tectonically induced subsidence during the Turonian and Campanian (Kölbel 1944; Voigt 1963; Baldschuhn et al. 1991). All layers were thus affected by subsidence, where the older units, that is, *Neocomian* and *Involutus Sandstones*, were buried deeper and the younger rocks, that is, *Heidelberg Sandstone*, were buried at shallower depths. Franzke et al. (2004) inferred the amount of subsidence of the eastern SCB to be $\sim$2 km during the Late Cretaceous, which yields burial depths for the *Involutus Sandstone* of $\sim$2.5–3 km and for the *Heidelberg Sandstone* of $<$2 km. Cataclasis, as found in the *Neocomian* and *Involutus Sandstones*, is thought to be the preferred deformation mechanism at depths of 1.5–2.5 km when rocks are lithified (Fossen et al. 2007). *Neocomian* and *Involutus Sandstones* are somewhat lithified, whereas most undeformed rocks in the SCB are poorly consolidated. The most active zone for cementation is thought to be at depths of 1–2 km but can occur as deep as 4–6 km (McBride 1989), consistent with the depth of burial of the *Heidelberg Sandstone*. Dissolution transfer is, however, independent from the depth of burial due to the influence of catalytic minerals. When clay minerals are present, dissolution transfer can take place at pressures significantly lower than the overburden load (Bjørkum 1996). On the other hand, higher pressures can influence the dissolution rates (Dewers and Hajash 1995), accelerating this process.

Although the inferred depths of burial of the *Involutus* and *Heidelberg Sandstones* appear to agree with those for cataclasis and cementation, respectively, their influence on deformation mechanism of the Subhercynian sandstones is only secondary. Rock-physical properties of the sandstones, such as variations in sorting and grain size, porosity and the presence or absence of mineral coatings and pore infilling, are found to have the highest impact on the deformation mechanisms. Furthermore, undeformed and horizontally bedded sands in the center of the Blankenburg Basin indicate that they have not undergone any major lithification. Despite similar depths of burial and the presence of catalytic minerals, these sandstones do not show any clay-induced dissolution, when compared to the steeply dipping counterparts. In the SCB dissolution, transfer is caused by pressure solution since it occurs within solution bands and stress-induced overgrowths at the flanks of the Blankenburg Basin, suggesting that it was primarily caused by tectonic stresses from the Harz Border Fault exerted on the sandstones.

This finding is also supported by the presence of undulose extinction (Fig. 8) and bulged grain boundaries with subgrain formation (Fig. 8b) in the heavily cemented part of the *Heidelberg Sandstone* (Fig. 2a, b), indicating high strain

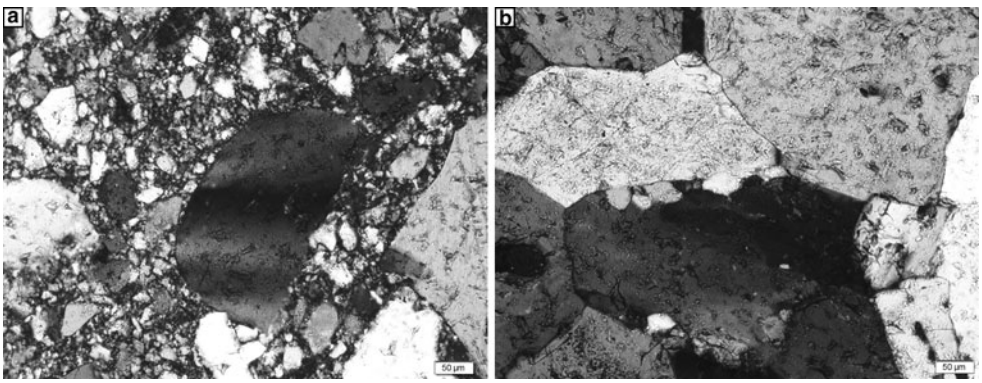

Fig. 8 Intracrystalline grain deformation. **a** Cross-polarized photomicrograph of cataclastically deformed *Involutus Sandstone* with a larger grain showing undulose extinction. **b** Cross-polarized photomicrograph of the quartz overgrows showing grains with irregular contacts and occurrence of subgrains forming at the edges of the internally more deformed crystal, indicated by undulose extinction

rates (Wu and Groshong 1991) in very low-grade metamorphic environments (Passchier and Trouw 2005). In the SCB, and especially in the steeply dipping and cemented parts of the *Heidelberg Sandstone*, these conditions were likely generated by the tectonic activity of the Harz Border Fault, making stress-induced quartz overgrowths a likely process to promote the cementation there.

Conditions for quartz overgrowths were found to be most favorable at 1,000–2,000 m or deeper burial depth at temperatures of 40–90 °C with slow cementation rates for subsurface sandstones (McBride 1989). However, these conditions pertain to isotropic overgrowth conditions and the effect of tectonic stresses acting on the grains was not taken into consideration. Water, especially in combination with stress state, can play an important role in the deformation of quartz. Water not only functions as a medium where silica can be dissolved, transported and precipitated in, it can also further complicate the deformation as its presence in the crystal lattice affects quartz crystal strength (Luan and Paterson 1992; Kronenberg 1994; Gleason and Tullis 1995; Kohlstedt et al. 1995; Post et al. 1996) and increased water pressure in the pore space between grains decreases their dislocation creep strength (Luan and Paterson 1992; Post et al. 1996).

Experiments on stress-induced rock-water interactions by Dewers and Hajash (1995) showed increased dissolution rates of quartz with increased pressures, temperatures and decreased grain sizes and also found quartz overgrowths at grain contact peripheries. Their results support the interpretation in this paper of an origin of the heavily cemented parts of the *Heidelberg Sandstone* from stress-induced quartz overgrowths in a water-saturated sandstone. Similar to faulted sandstones in the SCB, observations from the field along the Moab Fault, Utah, show sandstone cementation by quartz overgrowth accompanying the fault (Eichhubl et al. 2009). The origin of the cementation there is also linked to structural and diagenetic processes during faulting, referred to as structural diagenesis (Laubach et al. 2010). Microstructural observations and structural setting of the heavily cemented horizons in the *Heidelberg Sandstone* are also consistent with such structural diagenesis.

Stress-induced overgrowth mechanisms can explain the precipitation of quartz by diffusive mass transfer, as opposed to the previously suggested fluid convective processes. Silica-enriched fluids would not have to migrate over large distances, when silica can directly be dissolved and precipitated from nearby. Evidence for quartz dissolution is found within the cemented layers as well as in solution bands in adjacent layers. Voigt and Eynatten (2004, 2006) argue that the layers were uncompacted before cementation and that the origin of silica needs to be found elsewhere due to the undissolved appearance of the detrital grains. However, deformation bands found within these layers are overprinted by the cementation, indicating a localized compaction prior to the cementation. Furthermore, the anisotropic character of the overgrowths allows for the layers to appear less compacted in certain directions, depending on the stresses acting on the rocks.

Regardless of the driving mechanisms for the cementation, neither diffusive nor convective processes alone can sufficiently explain the amount of cement in the Santonian sandstones being precipitated within the time frame of tectonic activity and active basin formation. Nearby almost horizontal Lower Campanian layers indicate that the major tectonic movements and basin formation had ceased by then. Most studies that have quantified the timing of cementation show that time needed to form at least 5 % quartz cement can range from 1.6 to more than 50 Ma (McBride 1989). However, faster rates are reported from Dutton and Land (1988) where 900–1,500 m buried sandstones formed up to 30 % cement in 6 Ma and also from Haszeldine et al. (1984) who found up to 25 % cement in a time frame of only 1.6 Ma of >1,000 m buried sandstones. These fast rates are associated with elevated temperatures of 55–94 °C. Similar rates and conditions will also be needed at the SCB in order to explain the amount of cement in such a short time. In addition, Lander et al. (2008) conclude from laboratory synthesis of quartz overgrowths that cementation rates are slowed for coated grains as opposed to artificially cleaned grains, which is in support of the heavy cementation being so predominant in the horizons void of clay minerals and iron oxides of the *Heidelberg Sandstone*.

In order to obtain more detailed information on the nature, amount and timing of the cement of the sandstone towers, further studies in terms of depths of burial, crystallization temperatures of quartz by fluid inclusion, cathodoluminescence microscopy of oriented samples and the mutual influence of water, temperature, pressure and catalytical minerals on cementation would be needed. Nevertheless, our results suggest that the quartz cementation is of tectonic origin and likely be caused by stress-induced quartz overgrowths.

Conclusions

Structural analyses of deformed sandstone beds in the SCB show that the extent of the segments of the Teufelsmauer and the fracture geometries contained within these segments are all consistent with a deformation band damage zone accompanying the Harz Border fault. Within the Harz border fault damage zone, a suite of deformation mechanisms, all resultant from tectonic forces during damage zone formation, was found responsible for porosity reduction, development of deformation bands and the

heavy cementation. The spatial relationship of the fault damage zone with the geometry of the SCB, that is, rotating angular unconformities and overturned strata, is consistent with fault propagation folding as suggested by (Voigt et al. 2004) and confines the timing of the development of the deformation bands in a narrow time window between ~84 and ~83 Ma.

Moreover, the discovery of the deformation band damage zone in the SCB and mapping its extent brings additional insights into the geometry and kinematics of the controversially discussed Harz border fault. Kinematics recorded by the deformation band arrays indicate that all segments of the Teufelsmauer are likely to have developed as one coherent damage zone and demonstrate a consistent sense of thrusting of deformation bands throughout all segments of the Teufelsmauer that is also compatible with the NE/SW shortening direction of the Harz border fault. Comparison of band orientations and stress field with those from bands in rocks of similar age, composition, consolidation and tectonic setting at the Orange quarry in the *Bassin du Sud-Est*, France, show a striking degree of consistency, both illustrating the evolution of deformation band arrays during shortening related to foreland folding and thrusting.

Acknowledgments We thank C. Wibberley, A. Torabi, F. Agosta, R. Greiling, and H. Fossen for reviews, or comments and discussions on earlier drafts of this paper. The assistance in arranging and shipping background literature from Germany by Dr. J. Mutterlose, Dr. B. Niebuhr and I. Rueckhardt is greatly appreciated. Further thanks go to our colleagues from the Department of Geodynamics and Geomaterials at the Geo Forschung Zentrum (GFZ), Potsdam for discussing ideas and also providing additional literature. Dr. J. McCormack and Dr. M. Ahmadiantehrani from University of Nevada, Reno, are thanked for support with the SEM sample preparation and execution. This work was supported in part by a grant to RAS from NASA's Planetary Geology and Geophysics Program. The authors thank ConocoPhillips for permission to publish this work.

References

Anderson EM (1942) The dynamics of faulting and dyke formation with application to Britain. Oliver and Boyd, Edinburgh

Antonellini M, Pollard DD (1995) Distinct element modeling of deformation bands in sandstone. J Struct Geol 17:1165–1182

Aydin A, Berryman JG (2010) Analysis of the growth of strike-slip faults using effective medium theory. J Struct Geol 32:1629–1642. doi:10.1016/j.jsg.2009.11.007

Baldschuhn R, Best G, Kockel F (1991) Inversion tectonics in the north-west German basin. In: Spencer AM (ed) Generation, accumulation and production of Europe's hydrocarbons, Special publication of the European Association of Petroleum Geoscientists 1. University Press, Oxford, pp 149–159

Bense VF, Van den Berg EH, Van Valen RT (2003) Deformation mechanisms and hydraulic properties of fault zones in unconsolidated sediments; the Roer Valley Rift System, The Netherlands. Hydrogeol J 11:319–332

Bjørkum PA (1996) How important is pressure in causing dissolution of quartz in sandstones? J Sediment Res 66:147–154

Blenkinsop TG (2000) Deformation microstructures and mechanisms in minerals and rocks. Kluwer Academic Publishers, Dordecht

Davis GH (1999) Structural geology of the Colorado Plateau regional of southern Utah, with special emphasis on deformation bands. Boulder Colorado, GSA Special Paper 342, pp 157

Davis GH, Bump AP, Garcia PE, Ahlgren SG (2000) Conjugate Riedel deformation band shear zones. J Struct Geol 22:169–190

De Boer RB, Nagtegaal PJC, Duyvis EM (1977) Pressure solution experiments on quartz sand. Geochim Cosmochim Ac 41:257–264

Dewers T, Hajash A (1995) Rate laws for water-assisted compaction and stress-induced water-rock interaction in sandstones. J Geophys Res 100:13093–13112

Du Bernard X, Eichhbul P, Aydin A (2002a) Dilation bands: a new form of localized failure in granular media. Geophys Res Lett 29:2176. doi:10.1029/2002GL015966

Du Bernard X, Labaume P, Darcel C, Davy P, Bour O (2002b) Cataclastic slip band distribution in normal fault damage zones, Nubian sandstones, Suez rift. J Geophys Res 107:B7. doi:10.1029/2001JB000493

Dutton SP, Land LS (1988) Cementation and burial history of a low-permeability quartzarenite, Lower Cretaceous Travis Peak Formation, East Texas. GSA Bull 100:1271–1282

Eichhubl P, Davatzes NC, Becker SP (2009) Structural and diagenetic control of fluid migration and cementation along the Moab fault, Utah. AAPG Bull 93:653–681

Engelder JT (1974) Cataclasis and the generation of fault gouge. GSA Bull 85:1515–1522

Exner U, Grasemann B (2010) Deformation bands in gravels: displacement gradients and heterogeneous strain. J Geol Soc Lond 167:905–913. doi:10.1144/0016-76492009-076

Flodin E, Prasad M, Aydin A (2003) Petrophysical constraints on deformation styles in Aztec Sandstone, southern Nevada, USA. Pure Appl Geophys 160:1589–1610

Fossen H, Bale A (2007) Deformation bands and their influence on fluid flow. AAPG Bull 91:1685–1700

Fossen H, Schultz RA, Shipton ZK, Mair K (2007) Deformation bands in sandstone: a review. J Geol Soc Lond 164:755–769

Franzke HJ (1990) Kinematische Studien an Störungskataklasiten des Harzes und Suberherzynen Beckens. Z Geol Wiss 18:390–397

Franzke HJ, Schmidt D (1995) Die mesozoische Entwicklung der Harznordrandstörung—Makrogefügeuntersuchungen in der Aufrichtungszone. Zentralblatt für Geologie und Paläonologie 1:1443–1457

Franzke HJ, Voigt T, von Eynatten H, Brix MR, Burmester G (2004) Geometrie und Kinematik der Harznordrandstörung, erläutert an Profilen aus dem Gebiet von Blankenburg. Geowiss Mitt 11:39–62

Franzke HJ, Voigt T, von Eynatten H (2005) Aufschlüsse am Königstein (Teufelsmauer) bei Neinstedt. In: Friedel CH, Lorenz A (eds) Vortrags und Exkursionstagung Harzgeologie 2005: Exkursionsführer und Veröffentlichungen der Deutschen Gesellschaft für Geowissenschaften, 227:38–39

Füchtbauer H (1967a) Der Einfluss des Ablagerungsmilieus auf die Sandstein-Diagenese im Mittleren Buntsandstein. Sediment Geol 1:159–179

Füchtbauer H (1967b) Influence of different types of diagenesis on sandstone porosity. 7th World Petroleum Congress 2, 353–369

Gleason GC, Tullis J (1995) A flow law for dislocation creep of quartz aggregates determined with the molten salt cell. Tectonophysics 247:1–23

Gratier J-P, Guiget R (1986) Experimental pressure solution—deposition on quartz grains: the crucial effect of the nature of the fluid. J Struct Geol 8:845–856

Haszeldine RS, Samson IM, Cornford C (1984) Quartz diagenesis and convective fluid movement; Beatrice Oilfield, UK North Sea. Clay Miner 19:391–402
Heald MT (1955) Stylolites in sandstones. J Geol 63:101–114
Heald MT, Larese RE (1974) Influence of coatings on quartz cementation. J Sediment Petrol 44:269–1274
Heald MT, Renton JJ (1966) Experimental study of sandstone cementation. J Sediment Petrol 36:977–991
Healy D, Jones RR, Holdsworth RE (2006) Three-dimensional brittle shear fracturing by tensile crack interaction. Nature 439:64–67. doi:10.1038/nature04346
Heimlich K (1956) Zur Stratigraphie und Tektonik des westlichen Quedlinburger Sattels (subherzynes Becken). Abhandlungen der Deutschen Akademie der Wissenschaften zu Berlin, Klasse fuer Chemie, Geologie und Biologie 1:1–35
Hinze C, Jordan H, Knoth W, Kriebel U (1998) Geologische Karte Harz. Geologisches Landesamt Sachsen-Anhalt, Halle/Saale, scale 1(100):000
Houseknecht DW (1988) Intergranular pressure solution in four quartzose sandstones. J Sediment Petrol 58:228–246
James WC, Wilmar GC, Davidson BG (1986) Role of quartz type and grain size in silica diagenesis, Nugget Sandstone, south-central Wyoming. J Sediment Petrol 56:657–662
Jamison WR, Stearns DW (1982) Tectonic deformation of Wingate Sandstone, Colorado National Monument. AAPG Bull 66:2584–2608
Johnson AM (1995) Orientations of faults determined by premonitory shear zones. Tectonophysics 247:161–238
Katz Y, Weinberger R, Aydin A (2004) Geometry and kinematic evolution of Riedel shear structures, Capitol Reef National Park, Utah. J Struct Geol 26:491–501
Klimczak C (2011) Processes of progressive deformation with applications to jointing faulting and fluid flow. Dissertation, University of Nevada, Reno
Klimczak C, Wittek A, Doman D, Riller UP (2007) Fold origin of the NE-lobe of the Sudbury Basin, Canada; evidence from heterogeneous fabric development in the Onaping Formation and the Sudbury igneous complex. J Struct Geol 29:1744–1756
Klimczak C, Soliva R, Schultz RA, Chery J (2011) Sequential growth of deformation bands in a multilayer sequence. J Geophys Res 116:B09209. doi:10.1029/2011JB008365
Kohlstedt DL, Evans B, Mackwell SJ (1995) Strength of the lithosphere; constraints imposed by laboratory experiments. J Geophys Res 100:17587–17602
Kölbel H (1944) Die tektonische und paläogeographische Entwicklung des Salzgitterer Gebietes. Abhandlungen des Reichamtes für Bodenforschung 207:1–100
König S, Wrede V (1994) Zur Tektonik der Harzränder. Z Dtsch Geol Ges 145:153–171
Kronenberg AK (1994) Hydrogen speciation and chemical weakening of quartz. Rev Mineral 29:123–176
Lander RH, Larese RE, Bonnell LM (2008) Toward more accurate quartz cement models: the importance of euhedral vs. non-euhedral growth rates. AAPG Bull 92:1537–1564
Laubach SE, Eichhubl P, Hilgers C, Lander RH (2010) Structural diagenesis. J Struct Geol 32:1866–1872
Lothe AE, Gabrielsen RH, Bjørnevoll-Hagen N, Larsen BT (2002) An experimental study of the texture of deformation bands; effects on the porosity and permeability of sandstones. Petrol Geosci 8:195–207
Luan FC, Paterson MS (1992) Preparation and deformation of synthetic aggregates of quartz. J Geophys Res 97:301–320
Main I, Mair K, Kwon O, Elphick S, Ngwenya B (2001) Recent experimental constraints on the mechanical and hydraulic properties of deformation bands in porous sandstones: a review. In: Holdsworth RE, Strachan RA, Magloughlin JF, Knipe RJ (eds), The nature and significance of fault zone weakening. Geol Soc London Spec Publ 186:43–63
Mandl G, de Jong LNJ, Maltha A (1977) Shear zones in granular material. Rock Mech 9:95–144
Marshak S, Mitra G (1988) Basic methods of structural geology, Prentice-Hall, Englewood Cliff, NJ, pp 448
Matheron G (1963) Principles of geostatistics. Econ Geol Bull Soc Econ Geol 58:1246–1266
McBride EF (1989) Quartz cement in sandstones; a review. Earth-Sci Rev 26:69–112
Oelkers EH, Bjørkum PA, Murphy WM (1996) A petrographic and computational investigation of quartz cementation and porosity reduction in North Sea sandstones. Am J Sci 296:420–452
Okubo CH, Schultz RA (2005) Evolution of damage zone geometry and intensity in porous sandstone: insight gained from strain energy density. J Geol Soc Lond 162:939–949
Okubo CH, Schultz RA (2006) Near-tip stress rotation and the development of deformation band stepover geometries in mode II. GSA Bull 118:343–348
Olsson WA, Lorenz JC, Cooper SP (2004) A mechanical model for multiply-oriented conjugate deformation bands. J Struct Geol 26:325–338
Passchier CW, Trouw RAJ (2005) Microtectonics. Springer, Heidelberg, p 366
Patzelt G (2003) Nördliches Harzvorland. Berlin/Stuttgart, Gebrüder Borntraeger, Sammlung Geologischer Führer, Band 50, pp 182
Pittman ED (1972) Diagenesis of quartz in sandstones as revealed by scanning electron microscopy. J Sediment Petrol 42:507–519
Post AD, Tullis J, Yund RA (1996) Effects of chemical environment on dislocation reep of quartzite. J Geophys Res 101:22143–22155
Rawling GC, Goodwin LB (2003) Cataclasis and particulate flow in faulted, poorly lithified sediments. J Struct Geol 25:317–331
Renard F, Ortoleva P, Gratier JP (1997) Pressure solution in sandstones: influence of clays and dependence on temperature and stress. Tectonophysics 280:257–266
Renton JJ, Heald MT, Cecil CB (1969) Experimental investigation of pressure solution of quartz. J Sediment Petrol 39:1107–1117
Riller U, Schwerdtner WM (1997) Mid-crustal deformation at the southern flank of the Sudbury Basin, central Ontario. GSA Bull 109:841–854
Saillet E, Wibberley CAJ (2010) Evolution of cataclastic faulting in high-porosity sandstone, Bassin du Sud-Est, Provence, France. J Struct Geol 11:1590–1608. doi:10.1016/j.jsg.2010.02.007
Schulschenk W (1930) Die Quadersandsteine des östlichen Abschnitts der subherzynen Kreidemulde. Leopoldina 6
Schultz RA, Balasko CM (2003) Growth of deformation bands into echelon and ladder geometries. Geophys Res Lett 20:2033. doi:10.1029/2003GL018449
Schultz RA, Siddharthan R (2005) A general framework for the occurrence and faulting of deformation bands in porous granular rocks. Tectonophysics 411:1–18
Schutjens PMTM (1991) Experimental compaction of quartz sand at low effective stress and temperature conditions. J Geol Soc Lond 148:527–539
Shipton ZK, Cowie PA (2001) Damage zone and slip-surface evolution over μm to km scales in high-porosity Navajo sandstone, Utah. J Struct Geol 23:1825–1844
Shipton ZK, Evans JP, Robeson K, Forster CB, Snelgrove S (2002) Structural heterogeneity and permeability in faulted eolian sandstone: implications for subsurface modelling of faults. AAPG Bull 86:863–883
Stackebrand W, Franzke HJ (1985) Klippen am "Großvater". In: Bankwitz P, Schwab M (eds) Exkursionsführer Rupturen VI: Bruchtektonische Prozesse am Harznordrand, die Bedeutung der Rupturen für die Strukturierung der Erdkruste. Gesellschaft Geologische Wissenschaften DDR, Berlin, p 41

Stackebrand W, Franzke HJ (1989) Alpidic reactivation of the Variscan consolidated lithosphere—The activity of some fracture zones in central Europe. Z Geol Wiss 17:699–712

Stackebrandt W (1983) Zum tektonischen Charakter der Harznordrandstoerung. The tectonic character of the northern Harz border fault system. Ver Zent Ph 77:187–193

Stackebrandt W (1986) Beiträge zur tektonischen Analyse ausgewählter Bruchzonen der Sybherzynen Senke und angrenzender Gebiete (Aufrichtungszone, Flechtinger Scholle). Ver Zent Ph 79, pp 81

Stearns DW, Jamison WR (1977) Deformation of sandstones over basement uplifts, Colorado National Monument. In: Veal HK (ed) Field conference—Rocky Mountain Association of Geologists, pp 31–39

Stephan HJ (1970) Zur Diagenese des Mittleren Buntsandsteins in Suedoldenburg (Niedersachsen). (Diagenesis of the middle Buntsandstein in south Oldenburg, Lower Saxony). Meyniana 20:39–82

Tiwari RN, Roy RN (1974) Sedimentpetrologische Untersuchungen an oberkretazischen Sandsteinen der Subherzynen Kreidemulde. Freiberg Forschungsh 301:27–135

Twiss RJ, Moores EM (2007) Structural geology, 2nd edn. Freeman and Company, New York

Torabi A, Fossen H (2009) Spatial variation of microstructure and petrophysical properties along deformation bands in reservoir sandstones. AAPG Bull 93:919–938

Underhill JR, Woodcock NH (1987) Faulting mechanisms in high porosity sandstones; New Red Sandstone, Arran, Scotland. In: Jones ME, Preston RMF (eds) Deformation of Sediments and Sedimentary Rocks. Geol Soc Spec Publ 29:91–105

Voigt E (1963) Über Randtröge vor Schollenrändern und ihre Bedeutung im Gebiet der Mitteleuropäischen Senke und angrenzender Gebiete. Z Dtsch Geol Ges 114:378–418

Voigt T, von Eynatten H (2004) Das Subherzyne Kreidebecken. In: Mutterlose J, Steffahn J (eds) Exkursionsführer: Die Kreide des Sunherzynen und östlichen Niedersächsischen Beckens.: Bochumer Geowiss Arb 4:1–52

Voigt T, von Eynatten H (2006) Kreidezeitliche Sedimente und Diskordanzen im Subherzynen Becken. Jber Mitt oberrhein geol Ver 88:305–343

Voigt T, Hv Eynatten, Franzke HJ (2004) Late Cretaceous unconformities in the Subhercynian Basin (Germany). Acta Geol Pol 54:673–694

Wibberley CAJ, Petit JP, Rives T (2000) Mechanics of cataclastic 'deformation band' faulting in high-porosity sandstone, Provence. CR Acad Sci Paris 331:419–425

Wibberley CAJ, Petit JP, Rives T (2007) The mechanics of fault distribution and localization in high-porosity sands, Provence, France. J Geol Soc Lond Spec Publ 289:19–46

Wu S, Groshong RH Jr (1991) Low-temperature deformation of sandstone, southern Appalachian fold-thrust belt. GSA Bull 103:861–875